Supplementary information

Ionic liquid dispersed PDMS/SWCNT/Ag@Ni hybrid composite for temperature and pressure sensitive smart electromagnetic shielding application

Prem Pal Singh, Ankita Mandal, Parna Maity, Bhanu Bhusan Khatua*

Materials Science Centre, Indian Institute of Technology Kharagpur, Kharagpur- 721302, India.

***Corresponding author**

Prof. B. B. Khatua (Email: khatuabb@matsc.iitkgp.ac.in)

Materials Science Centre, Indian Institute of Technology, Kharagpur – 721302, India

Tel.: +91- 3222-283982

1. Calculation of EMI SE and related parameters

1.1. EMI shielding

The ability to reduce the transmission of radiation is measured as the shielding effectiveness of materials given as decibel (dB). For all kinds of EMI shielding, mainly three shielding mechanisms reflection shielding (SE_R), absorption shielding (SE_A) and multiple reflection shielding (SE_M) contributed to total shielding (SE_T). Experimentally, SE_R, and SE_A are calculated from VNA generated scattering parameters (S_{11}, S_{12}, S_{21}, S_{22}) by utilizing the following equations (1S-6S):[1-4]

$$R = |S_{11}|^2 = |S_{22}|^2 \qquad (1S)$$

$$T = |S_{21}|^2 = |S_{12}|^2 \qquad (2S)$$

$$A + R + T = 1 \qquad (3S)$$

$$SE_R = -10\log_{10}(1-R) = -10\log_{10}\left(1-|S_{11}|^2\right) \qquad (4S)$$

$$SE_A = -10\log_{10}\left(\frac{T}{1-R}\right) = -10\log_{10}\left(\frac{|S_{12}|^2}{1-|S_{11}|^2}\right) \qquad (5S)$$

The total EMI SE (*EMI SE_T*) mathematically, can be expressed as:

$$EMI\,SE_T = SE_A + SE_R = -10\log_{10}(T) = -10\log_{10}|S_{21}|^2 \qquad (6S)$$

1.2. Green index (g_s)

This parameter reveals capability of shielding material to absorb the electromagnetic waves i.e. higher g_s higher the EM wave absorption ability.[3]

$$g_s = \frac{1}{R} - \frac{T}{R} - 1 \qquad (7S)$$

Here R and T are the reflection coefficient and transmission coefficient, were calculated from eq. 1S and 2S.

1.3. Eddy current loss

This loss in the shielding materials is caused by eddy currents generation and can be calculated using the following relationship:[4]

$$C_o = \frac{\mu''}{(\mu')^2 f} \qquad (8S)$$

Where f is the frequency (Hz), μ’ and μ’’ are the real and imaginary magnetic permeability.

1.4. DC conductivity calculation

$$\sigma_{DC} = \frac{L}{RA}(S/cm) \qquad (9S)$$

Where L is the length, A is the cross-sectional area, and R is the resistance (Ω).

2. Ag@Ni particle size distribution and contact angle of water on surface PDMS film

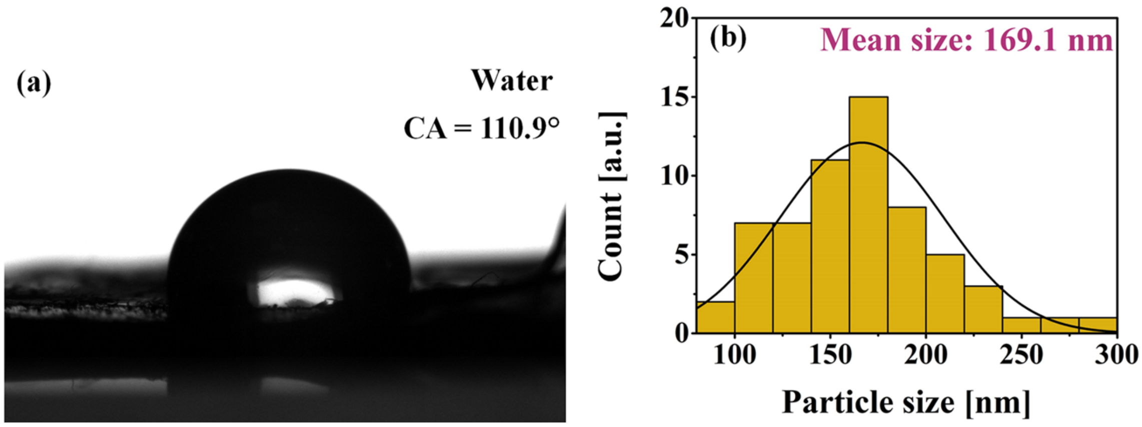

Fig. 1. (a) histogram of Ag@Ni particle size distribution, (b) contact angle of water with PDMS film surface.

Table 1. Summary and labeling of 3M IL containing composites, without IL-impregnated composites.

Composite system	**Description**	**Average sample thickness**
NaCl	18.45 wt.% of 3M NaCl water ionic liquid entrapped in PDMS	2.37
$CaCl_2$	18.2 wt.% of $CaCl_2$/water ionic liquid entrapped in PDMS	2.36
KI	18.61 wt.% of KI/ water ionic liquid entrapped in PDMS	2.36
S1	PDMS/SWCNT(0.5 wt.%)	2.38
S2	PDMS/Ag@Ni(1 wt.%)/SWCNT(0.5 wt.%)	2.37

3. Elemental composition and elemental mapping of Ag@Ni nanoparticles

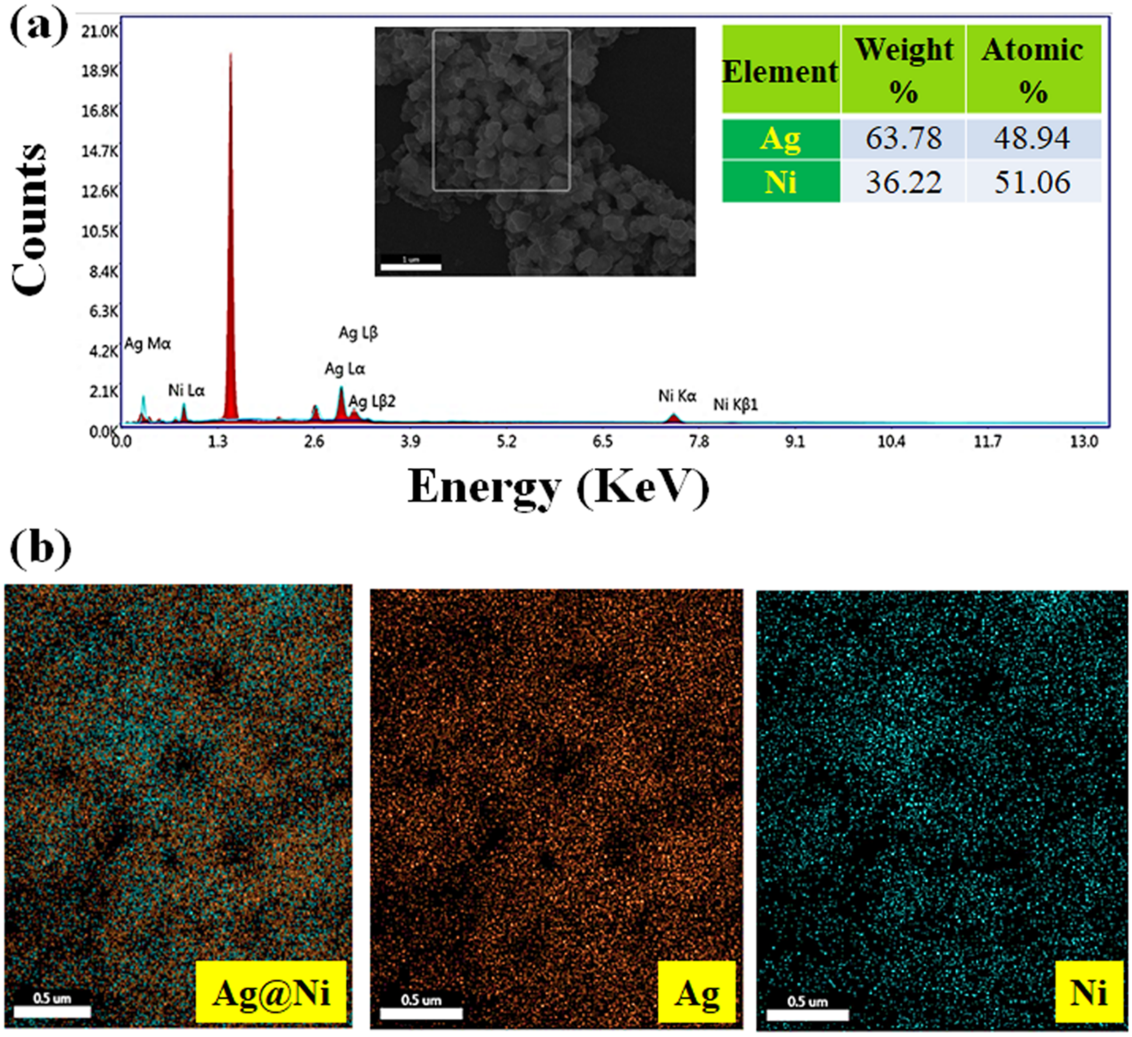

Fig. 2. (a) EDS spectrum of Ag@Ni nanoparticles, (b) EDS elemental mapping of Ag@Ni.

4. Elemental composition and elemental mapping on surface of KIL3F composite

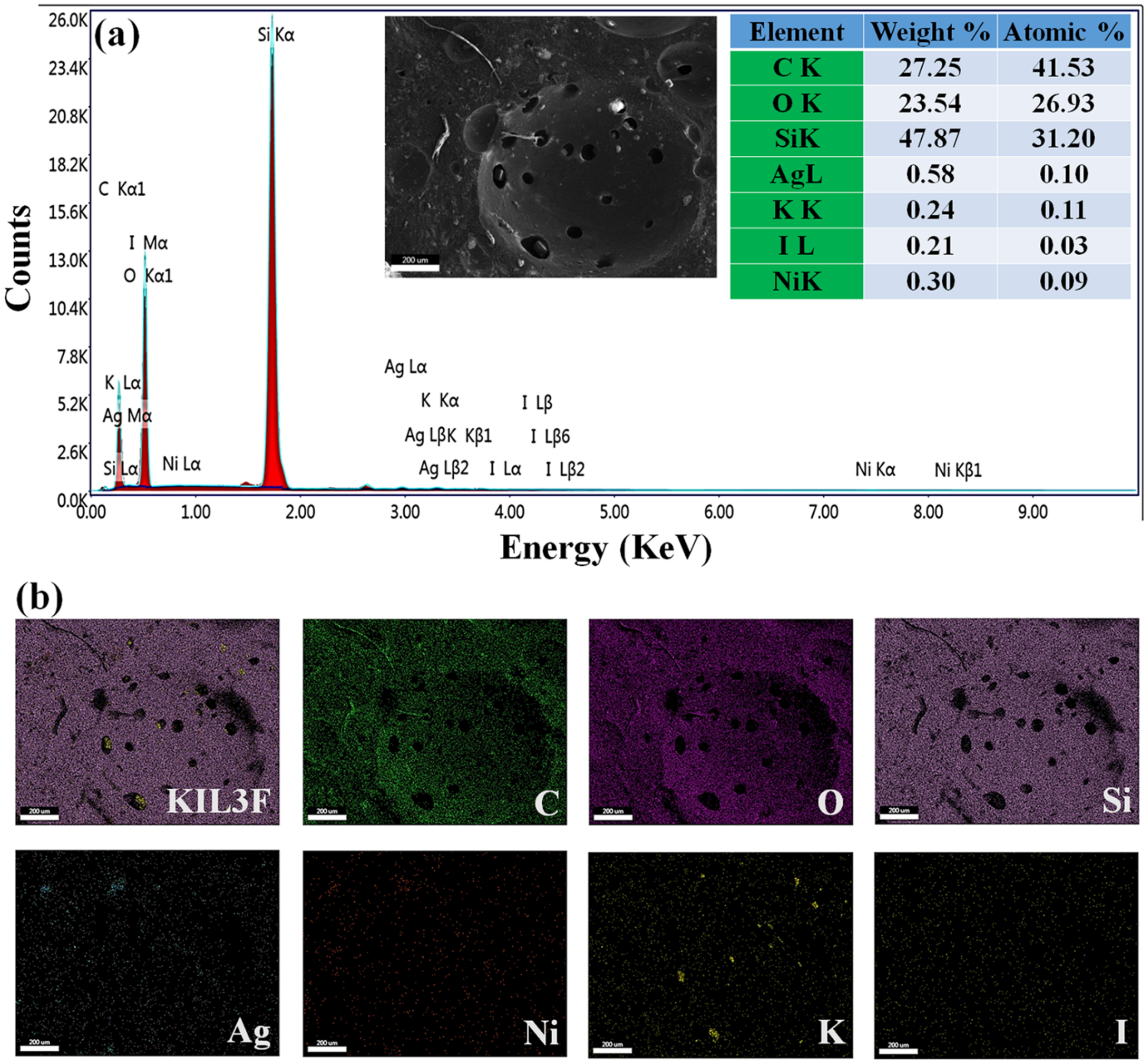

Element	Weight %	Atomic %
C K	27.25	41.53
O K	23.54	26.93
SiK	47.87	31.20
AgL	0.58	0.10
K K	0.24	0.11
I L	0.21	0.03
NiK	0.30	0.09

Fig. 3. (a) EDS spectrum of KIL3F composite surface, (b) elemental distribution (mapping) in the KIL3F surface.

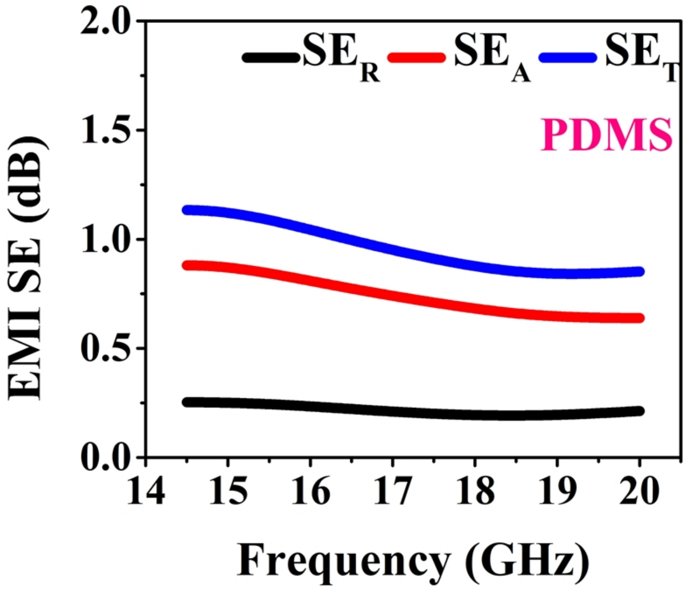

Fig. 4. Reflection, absorption and total shielding performance of the 1.84 mm thick PMDS film.

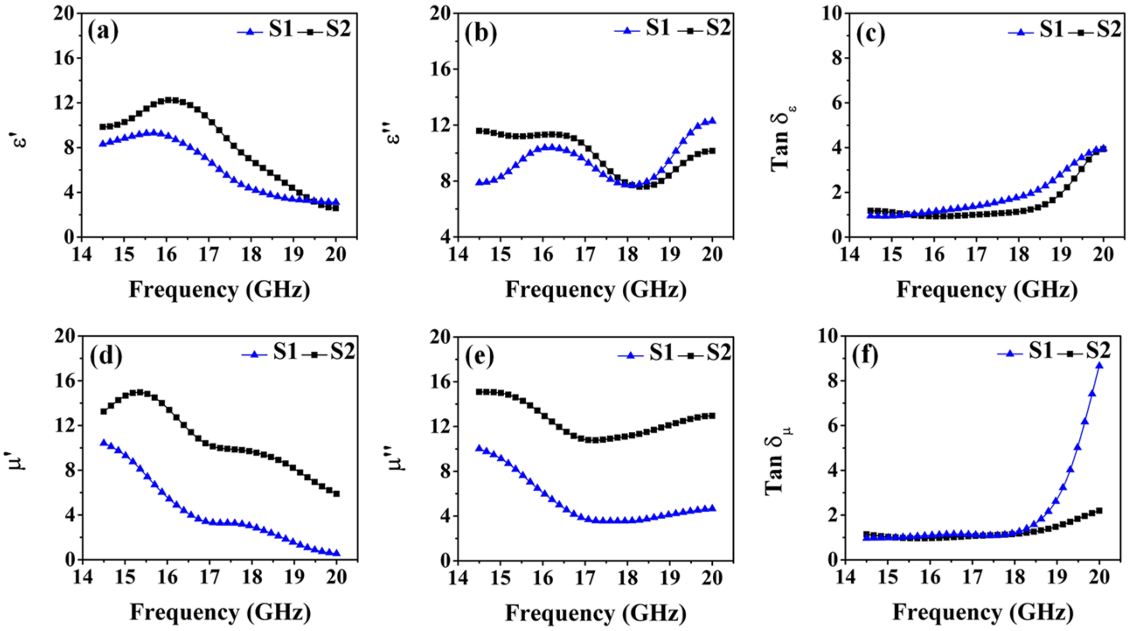

Fig. 5. (a) real permittivity, (b) imaginary permittivity, (c) dielectric loss tangent, (d) real permeability, (e) imaginary permittivity, and (f) magnetic loss tangent of S1 and S2 composites (as labeled in table 1, above).

5. Calculation of complex permittivity and complex permeability

5.1. Complex permittivity

$$\varepsilon^{*} = \varepsilon^{'} + i\varepsilon^{''} \tag{10S}$$

Magnitude:

$$\varepsilon^{*} = \sqrt{\left(\varepsilon^{'}\right)^{2} + \left(\varepsilon^{''}\right)^{2}} \tag{11S}$$

5.2. Complex permeability

$$\mu^{*} = \mu^{'} + i\mu^{''} \tag{12S}$$

Magnitude:

$$\mu^{*} = \sqrt{\left(\mu^{'}\right)^{2} + \left(\mu^{''}\right)^{2}} \tag{13S}$$

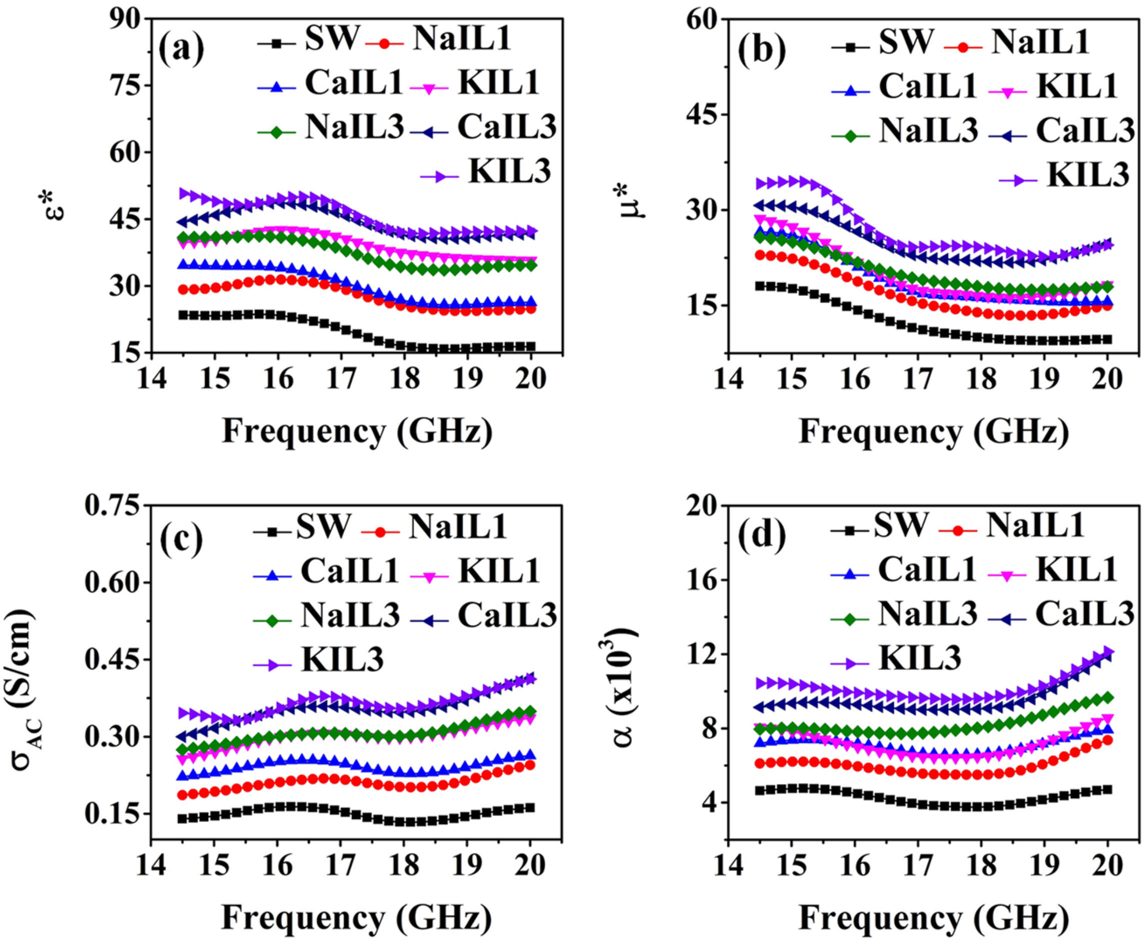

Fig. 6. (a) complex dielectric permittivity, (b) complex magnetic permeability, (c) AC conductivity (conduction loss), and (d) attenuation constant of IL entrapped composites as labeled in table 1 in the main text.

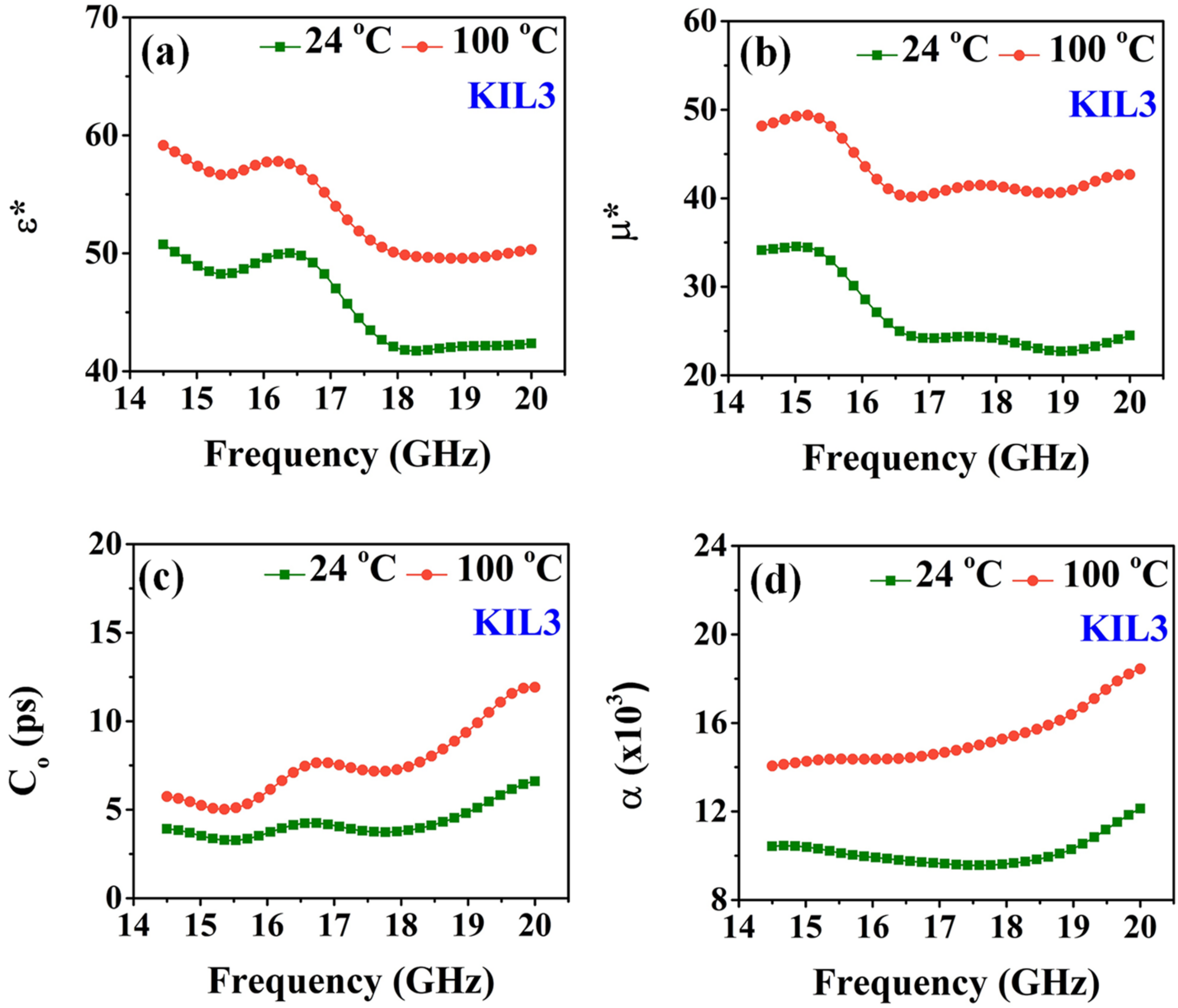

Fig. 7. temperature and frequency dependent: (a) complex dielectric permittivity, (b) complex magnetic permeability, (c) eddy current loss, and (d) attenuation constant of KIL3 composite (as labeled in table 1 in the main text).

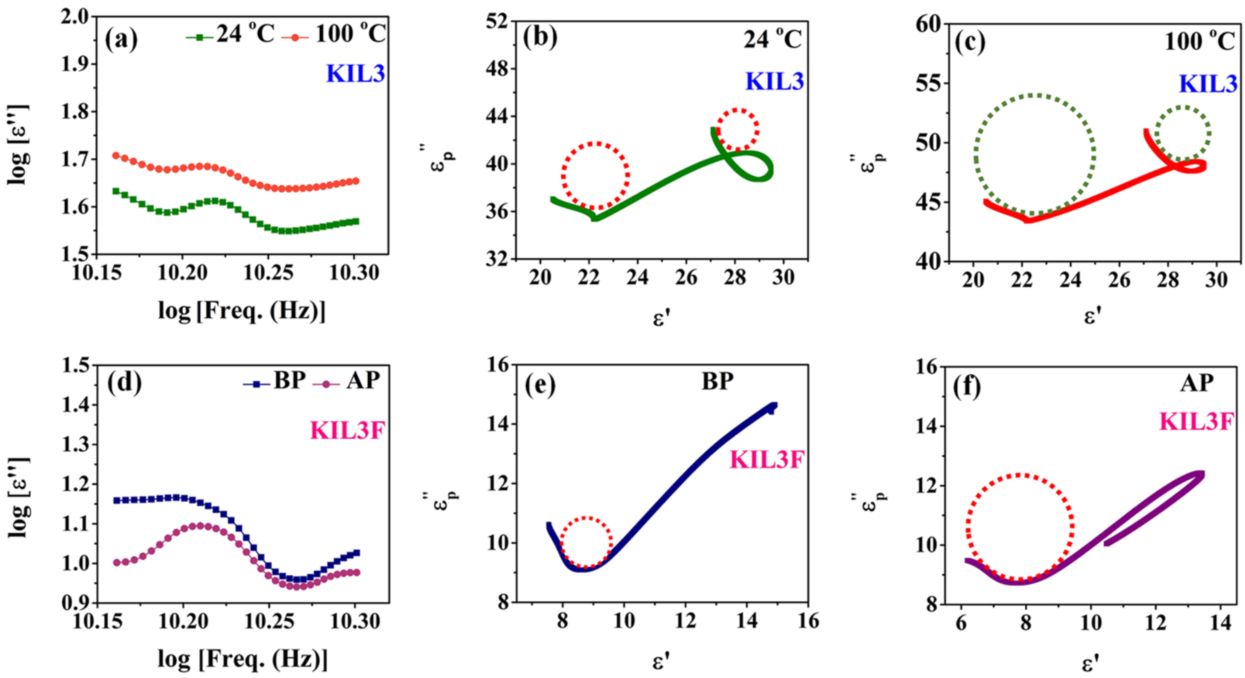

Fig. 8. thermally tuned (a) log-log plot of imaginary permittivity against frequency at 24 °C and 100 °C in KIL3, (b, c) polarization loss at 24 °C and 100 °C in KIL3, and pressure induced (d) log-log plot of imaginary permittivity against frequency before pressing (BP) and after pressing (AP) in KIL3F, (e, f) polarization loss before pressing (BP) and after pressing (AP) in KIL3F.

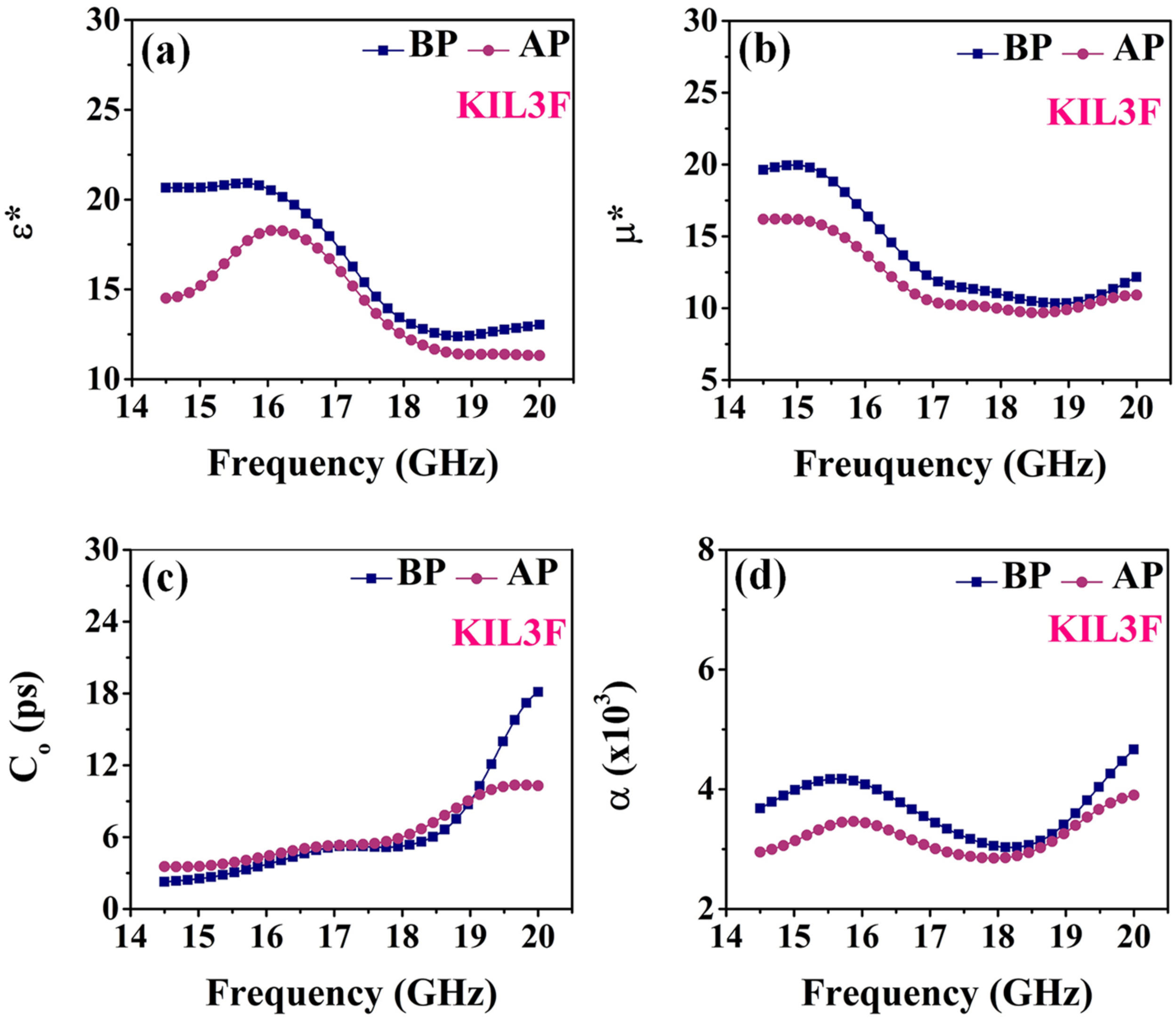

Fig. 9. pressure and frequency dependent: (a) complex dielectric permittivity, (b) complex magnetic permeability, (c) eddy current loss and (d) attenuation constant of IL generated foamed KIL3F composite (as labeled in table 1 in the main text).

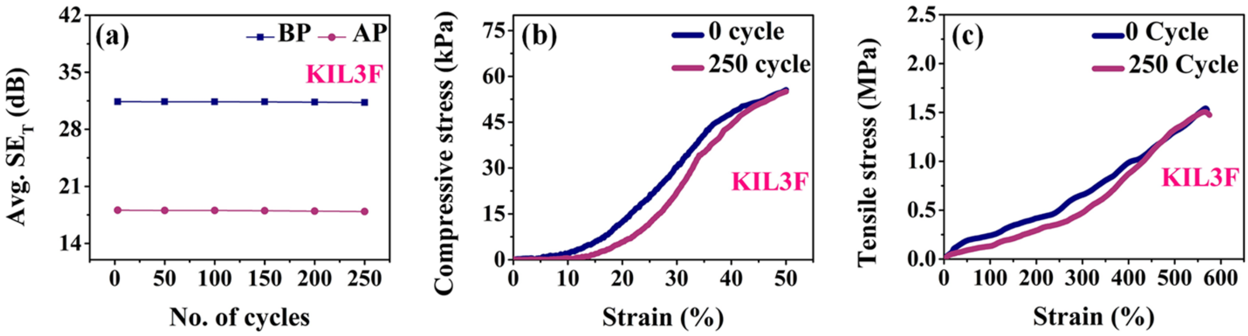

Fig. 10. (a) cyclic stability of shielding performance of KIL3F composite before and after 250 manual compression and relaxation cycles, (b) compressive stress vs. compressive strain curve of KIL3F composite before and after 250 manual compression and relaxation cycles, (c) tensile stress-strain curve of KIL3F composite before and after 250 manual compression and relaxation cycles.

References

1. A. De, S. Paria, A. Bera, S.K. Si, S. Bera and B.B. Khatua, ACS Appl. Engi. Mater., 2023, 1, 95–108.

2. R. Bera, A. Maitra, S. Paria, S.K. Karan, A.K. Das, A. Bera, S.K. Si, L. Halder, A. De and B.B. Khatua, Chem. Engi. J., 2018, 335, 501-509.

3. X. Jia, Y. Li, B. Shen and W. Zheng, Compos. P-B: Engi., 2022, 14, 109652.

4. C. Wang, V. Murugadoss, J. Kong, Z. He, X. Mai, Q. Shao, Y. Chen, L. Guo, C. Liu, S. Angaiah and Z. Guo, Carbon, 2018, 140, 696-733.